HHS Public Access

Author manuscript

Dev Cell. Author manuscript; available in PMC 2017 January 25.

Published in final edited form as:

Dev Cell. 2016 January 25; 36(2): 215–224. doi:10.1016/j.devcel.2015.12.018.

An NF-κB – EphrinA5 – Dependent Communication between NG2+ Interstitial Cells and Myoblasts Promotes Muscle Growth in Neonates

Jin-Mo Gu[1,2,3,4], **David J. Wang**[1,4], **Jennifer M. Peterson**[1,2,4], **Jonathan Shintaku**[1,2,3,4], **Sandya Liyanarachchi**[4], **Vincenzo Coppola**[1,4], **Ashley E. Frakes**[5], **Brian K. Kaspar**[5], **Dawn D. Cornelison**[6], and **Denis C. Guttridge**[1,2,3,4,*]

[1]Department of Molecular Virology, Immunology, and Medical Genetics, Columbus, Ohio 43210

[2]Center for Muscle Health and Neuromuscular Disorders, Columbus, Ohio 43210

[3]Molecular, Cellular and Developmental Biology Graduate Program, Columbus, Ohio 43210

[4]The Ohio State University Medical Center, Columbus, Ohio 43210

[5]Nationwide Children's Hospital, Columbus, Ohio 43205, USA

[6]Division of Biology and Bond Life Sciences Center, University of Missouri, Columbia, Missouri, 65203, USA

SUMMARY

Skeletal muscle growth immediately following birth is a critical for proper body posture and locomotion. However, compared to embryogenesis and adulthood, the processes regulating the maturation of neonatal muscles is considerably less clear. Studies in the 1960s predicted that neonatal muscle growth results from nuclear accretion of myoblasts preferentially at the tips of myofibers. Remarkably, little information has been added since then to resolve how myoblasts migrate to the ends of fibers. Here, we provide insight to this process by revealing a unique NF-κB-dependent communication between $NG2^+$ interstitial cells and myoblasts. NF-κB in $NG2^+$ cells promotes myoblast migration to the tips of myofibers through cell-cell contact. This occurs through expression of ephrinA5 from $NG2^+$ cells, which we further deduce is an NF-κB target gene. Together, results suggest that NF-κB plays an important role in the development of newborn muscles to ensure proper myoblast migration for fiber growth.

* Correspondence: denis.guttridge@osumc.edu.

ACCESSION NUMBERS

The accession numbers for the data of microarray and RNAseq shown in this paper are GSE75774 and GSE75832, respectively.

AUTHOR CONTRIBUTION

J-M.G. designed, performed, and analyzed the experiments. J.W., J.M.P, and J.S. assisted in optimizing FACS conditions and *in vivo* mouse experiments. S.L. performed the bioinformatics analysis for the array data. V.C. generated *Efna5*$^{tm1a/+}$ mice. B.K. and A.F. helped to optimize the live cell imaging experiment. D.D.C. contributed to discussion. J-M.G. wrote and helped with the editing phase of the manuscript. D.C.G supervised, designed experiments, and contributed to the editing of the manuscript.

Keywords

NF-κB; ephrinA5; skeletal muscle; myoblast; migration; development

INTRODUCTION

In humans, the growth of an infant in the first 1000 days of life is considered vital for maximizing cognitive and behavioral function, as well as minimizing the risk of chronic diseases later in life (Britto and Perez-Escamilla, 2013). The rate at which neonates grow is higher than in any other stage of postnatal development, and the majority of this growth, as measured in mass, derives from skeletal muscle (Davis and Fiorotto, 2009). Surprisingly, in contrast to the wealth of studies that have been devoted to elucidating the development of skeletal muscle during embryogenesis, and the response to injury in adults, little attention has been given to the maturation of newborn muscles.

Following birth, the total number of myofibers are thought to remain fixed throughout adulthood (White et al., 2010). Rather than adding myofibers, muscles grow longitudinally through the accretion of myoblasts, resulting in an increasing pool of myonuclei that regulate the synthesis of contractile proteins and the addition of sarcomeric units (Braun and Gautel, 2011; Ehler and Gautel, 2008). The growth of these fibers is important to support a musculoskeletal apparatus needed for locomotion and posture. In mice, this post-embryonic growth phase is complete by the third week of life (White et al., 2010). Further growth of muscle fibers results from an increase in protein synthesis due to the uptake of nutrients (Davis and Fiorotto, 2009). Early tracer studies postulated that the location where myoblasts fuse along the length of a myofiber is not a random process, but rather a coordinated event occurring at the tip of the fiber (Kitiyakara and Angevine, 1963; Williams and Goldspink, 1971). Nevertheless, how myoblasts from the interstitium receive their cues to migrate to the correct position on the fiber has yet to be identified. In this study we describe a mechanism involving the NF-κB signaling pathway and an intimate communication between an interstitial cell population and myoblasts that together coordinate neonatal muscle growth.

RESULTS

NF-κB is Activated in NG2$^+$ Cells during Neonatal Muscle Development

We previously showed that limb muscles from newborn mice contain a considerably high level of NF-κB activity, composed of the classical p50 and p65 subunits in the signaling pathway (Dahlman et al., 2010; Hayden and Ghosh, 2004, 2012). To identify a cellular source for this activity, we used reporter mice whose EGFP expression in the cytoplasm is under the control of an NF-κB regulated promoter (*NFκB-EGFP*) (Magness et al., 2004). Results showed that NF-κB activity was localized to the muscle interstitium and declined rapidly throughout the first 4 weeks of life, coinciding with the growth plateau phase of neonatal limb muscles (Figure 1A). Reporter mice also revealed that a significant portion of NF-κB activity in the extra laminar space was localized to a population distinct from Pax7$^+$ or MyoD$^+$ myogenic cells (Figure 1B).

Fluorescence-activated cell sorting (FACS) analysis was used to characterize those populations positive for NF-κB within neonatal muscle. Results showed that a major fraction of activity resided in both $NG2^+$ (23.0 ± 2.3%) and $CD31^+$ (18.0 ± 4.9%) cells, with less activity present in cells positive for F4/80, PDGFRα, or ER-TR7 markers (Figure 1C). While CD31 is present on endothelial cells, NG2 is expressed on the surface of pericytes and other cell types (Cappellari and Cossu, 2013). Immunohistochemical staining of P7 hindlimb muscles verified that cells positive for NF-κB co-localized with cells expressing NG2 and CD31 (Figure 1D). In neonatal muscle, alkaline phosphatase (AP) also serves as a marker for pericytes (Dellavalle et al., 2011). However, only a minor portion of GFP^+ cells was positive for AP (<1.5%), and rarely did AP^+ cells appear in the same population as $NG2^+$ cells (Figure S1A). In addition, and consistent with FACS results, rarely did we observe cells positive for both NF-κB and AP (Figure S1B). Similar results were obtained for another pericyte marker, PDGFRβ (Figure 1C). These data demonstrate that, in newborn muscle, NF-κB predominantly resides in both endothelial cells and an interstitial $NG2^+$ population that appears distinct from pure pericytes.

NF-κB Functions in $NG2^+$ Cells to Promote Myoblast Migration Through Cell-Cell Contact

To investigate the functional role of $CD31^+$ and $NG2^+$ cells during neonatal muscle growth, we established co-cultures of these cells with C2C12 myoblasts stably expressing a H2B-GFP reporter gene. This system allowed us to monitor myoblasts over time using fluorescent, live cell imaging. A clear difference was observed in the motility of myoblasts when co-cultured with $NG2^+$ but not $CD31^+$ cells, which could not be accounted for by differences in proliferation rates, as monitored by Ki67 staining (movie S1, and Figure S1C). Co-culture studies also revealed that $NG2^+$ cells and myoblasts underwent cell-cell contact. Tracking of cell movements showed that myoblasts were 33% ($p = 0.0023$) more mobile in the presence of $NG2^+$ compared to $CD31^+$ cells (Figure 1E), suggesting that cell-cell contact likely contributed to the increased motility of myoblasts. Further tracking examination revealed that following cell contact, myoblasts tended to migrate away from $NG2^+$ cells (Figure 1F) indicating that the movement of myoblasts results from contact-mediated repulsion. To further assess the migration stimulating activity of $NG2^+$ cells, Boyden chambers were used so that C2C12-H2B:GFP myoblasts could be grown either in the same well as $NG2^+$ cells, or separated by a transwell filter (Figure 1F). Compared to the migration of C2C12-H2B:GFP myoblasts when plated by themselves (set to a value of 1), the addition of $NG2^+$ cells in a separate well had no effect on myoblast migration. In contrast, combining the two cell types in the same well promoted C2C12-H2B:GFP myoblasts migration through the filter (Figure 1F). This strongly suggested that $NG2^+$ cells function to stimulate myoblast motility through cell-cell contact rather than through a diffusible factor.

Since we found that NF-κB is active in $NG2^+$ cells within newborn muscles, we next asked whether this activity is required for myoblast migration. Thus, co-culture assays were repeated with C2C12-H2B:GFP myoblasts and $NG2^+$ cells genetically ablated for the p65 subunit of NF-κB. Results showed that myoblasts favored contacting $p65^{+/+}$ $NG2^+$ cells, which associated with a 47% ($p = 0.0352$) increase in myoblast motility compared to co-cultures with $p65^{-/-}$ $NG2^+$ cells (movie S2 and Figure 2A). To substantiate these results, we

performed a separate migration assay using a two-chamber system, which, as illustrated in Figure 2B, allows the simultaneous culture of two distinct cell populations in the same culture dish. Unlabeled C2C12 myoblasts were plated in one chamber and subsequently differentiated into myotubes prior to plating a mixture of C2C12-H2B:GFP myoblasts with $p65^{+/+}$ or $p65^{-/-}$ $NG2^{+}$ cells in the opposite chamber. Following the removal of a gasket separating the chambers, we quantitated the number of C2C12-H2B:GFP myoblasts that migrated across the gap in the direction of differentiated myotubes. Results showed that myoblast migration was considerably increased by 209% ($p = 0.00683$) in the presence of $p65^{+/+}$ $NG2^{+}$ cells compared to $p65^{-/-}$ $NG2^{+}$ cells (Figure 2B and movie S3). This regulation was selective to the p65 subunit, since similar differences in myoblast migration were not observed between $p50^{+/+}$ and $p50^{-/-}$ $NG2^{+}$ cultures (Figure S2A). We also found that migration was more efficient when myoblasts were exposed to myotubes rather than an empty chamber (Figure S2B), consistent with the notion that myotubes secrete chemotactic factors to stimulate myoblast motility (Griffin et al., 2010). We previously demonstrated that p65 regulation of the inducible nitric oxide synthase gene (iNOS) and secretion of nitric oxide (NO) from stromal fibroblasts promotes myoblast nuclear accretion to myofibers (Dahlman et al., 2010). To determine whether this regulation was also relevant in myoblast migration, we repeated migration assays in the presence of NO. However, neither the NO donor, sodium nitroprusside (SNP), or $iNOS^{-/-}$ $NG2^{+}$ cells had a significant effect on the migration of C2C12-H2B:GFP myoblasts, suggesting that p65 regulation of iNOS is not involved in mobilizing skeletal muscle cells (Figure S2C and S2D).

NF-κB Functions in $NG2^{+}$ Cells to Promote Myoblasts Migration *in vivo*

Next, we asked if NF-κB controls myoblast migration *in vivo*. Mice containing an *CreERT2* allele under the control of the NG2 promoter were crossed with $p65^{flox/flox}$ ($p65^{fl/fl}$) mice (Steinbrecher et al., 2008). Resulting progenies with genotypes $NG2^{CreER};p65^{+/+}$ and $NG2^{CreER};p65^{fl/fl}$ were administered tamoxifen at P2 to induce Cre-mediated deletion of p65 in NG2 cells. Hindlimb muscles were subsequently analyzed at P30, when postnatal muscle development is stabilized. No differences were observed in myofiber number per area (Figure S2E). However, we noted that the number of myonuclei per fiber were significantly reduced in $NG2^{CreER};p65^{fl/fl}$ mice, coinciding with an increase in the number of cells residing in the muscle interstitium (Figure 2C and 2D). In addition, we observed an unusual heterogeneity in myofiber size in $NG2^{CreER};p65^{fl/fl}$ mice compared to $NG2^{CreER};p65^{+/+}$ mice (Figure 2E).

Results above are consistent with our *in vitro* data supporting the hypothesis that p65 functions in $NG2^{+}$ cells to regulate migration of myoblasts to their target myofibers. We then performed an *in vivo* myoblast migration assay adopted from earlier studies. This technique depends on DNA analogues to track dividing cells in newborn muscles, and was originally used to demonstrate that the accretion of myoblasts to growing myofibers preferentially occurs at the ends of the fibers (Kitiyakara and Angevine, 1963; Williams and Goldspink, 1971). As illustrated in Figure 2F, when this approach was performed by pulsing hindlimbs of P2 mice with the thymidine analogue, 5-bromo-2-deoxyuridine (BrdU), the position of $BrdU^{+}$ nuclei in extensor digitorum longus (EDL) muscles could be tracked over time due to the sequential accretion of unlabeled myoblasts. For example, by serial cross

section and whole-mount analysis of EDL muscles, $BrdU^+$ myonuclei were positioned closer to the midline at P21 compared to P14 (Figure S2F), which supports the model that the fusion of myoblasts to a growing myofiber is coordinated in a spatial rather than in a random process. We proceeded to use the same labeling strategy with P2 $NG2^{CreER};p65^{+/+}$ and $NG2^{CreER};p65^{fl/fl}$ mice injected with BrdU and tamoxifen. $BrdU^+$ myonuclei were subsequently scored from EDL muscle sections. Results showed that the number of $BrdU^+$ myonuclei localized at the midline of EDL muscles was significantly reduced by 87% ($p = 0.00533$) in $NG2^{CreER};p65^{fl/fl}$ compared to $NG2^{CreER};p65^{+/+}$ mice (Figure 2G, 2H, and S2G). Whole-mount muscle analysis showed that this difference was not due to any changes to the position of $NG2^+$ cells along the length of the myofiber resulting from p65 deletion (Figure S2H). Taking into account both *in vitro* and *in vivo* results, these findings strongly support the notion that in newborn muscles, NF-κB functions in $NG2^+$ cells to stimulate the migration of myoblasts to the tips of myofibers for accretion to occur.

EFNA5 is Directly Regulated by NF-κB Signaling

To gain insight into the mechanism by which NF-κB functions in this capacity, we performed genome wide expression profiling using microarray and RNA Seq analyses from early (P2), mid (P7), and late (P14) time points of neonatal muscle development. Annotation from both methods revealed the predicted regulatory expression changes in fetal and neonatal myosin genes (Figure S3A and S3B). We then mined for candidate genes involved in cell migration whose protein function is dependent on cell-cell contact. One class of genes that fit this criterion was the Eph/Ephrin receptor tyrosine kinase family, which function by transmitting their signals between ligand (Ephrin) and receptor (Eph) to promote directional migration (Petrie et al., 2009; Poliakov et al., 2004). Interestingly, several Eph/Ephrin members have been described to regulate skeletal muscle progenitor cell motility (Li and Johnson, 2013; Siegel et al., 2009; Stark et al., 2011; Swartz et al., 2001). Both microarray and RNA Seq revealed that several of the Eph/Ephrin genes (*EFNA2*, *EFNA4*, *EFNA5*, *EFNB1*) were down regulated in hindlimb muscles during the first two weeks of life, results that we validated by quantitative RT-PCR analysis (Figure 3A). Since this gene expression pattern was consistent with what we had earlier observed for NF-κB activity (Figure 1A), we considered that Eph/Ephrin genes might be transcriptional targets of NF-κB. We therefore used the rVista database to query Eph/Ephrin promoters for potential NF-κB regulatory elements. One gene, *EFNA5*, contained conserved NF-κB binding sites at positions −2969, −1480, and +163, relative to the transcriptional start site (Figure 3B). Chromatin immunoprecipitation experiments in $NG2^+$ cells confirmed the binding of p65 to each of these sites, which were enriched in response to an NF-κB inducer (IL-1β, Figure 3C). Similar binding of p65 to *EFNA5* was observed in $p65^{+/+}$ mouse embryonic fibroblasts (MEFs), which as expected was pronouncedly reduced in $p65^{-/-}$ cells (Figure 3D). We next tested the functionality of this site by generating a luciferase reporter construct containing the wild type and mutated version of the +163 NF-κB binding site. Results showed that the *EFNA5* reporter was active in MEFs, but this activity was significantly diminished when assays were repeated with a mutated NF-κB binding site (Figure 3E). Such results provided evidence that the *EFNA5* gene is a direct target of NF-κB. For further validation, we tested the expression of *EFNA5* in $NG2^+$ cells by FACS analysis. *EFNA5* expression was significantly reduced in $p65^{-/-}$ compared to $p65^{+/+}$ $NG2^+$ cells (Figure 3F). Similar results

were obtained with $p65^{+/+}$ and $p65^{-/-}$ MEFs (Figure S3C), which together demonstrated that expression of *EFNA5* in neonatal muscle is under NF-κB control.

EphrinA5 is a Regulator of Myoblast Migration

Next, we assessed the functional relevance of *EFNA5* in myoblast migration by using a Boyden chamber assay. C2C12 myoblasts were cultured in the upper well and subsequently treated with eight different types of recombinant Fc-clustered ephrin ligands (ephrinA1–A5 and ephrinB1–B3). Whereas some myoblast migratory activity was observed from ephrinA1-Fc and A2-Fc, the greatest stimulation came from ephrinA5-Fc (Figure 4A). To confirm this specificity to *EFNA5*, C2C12-H2B:GFP myoblasts were co-cultured with MEFs that had been previously transfected with an siRNA against *EFNA5* (Figure S4A) and myoblast migration was monitored in a two chamber migration system as described in Figure 2. Knockdown of *EFNA5*, but not siControl or an siRNA against *EFNB1*, caused a significant reduction in myoblast motility (Figure 4B and S4B).

To determine if a similar function for *EFNA5* could be recapitulated *in vivo*, we generated conditional mutant mice using a targeting vector where exon 2 of *EFNA5* was flanked by flox alleles (Figure S4C). These mice were crossed with $NG2^{CreERT2}$ mice to generate $NG2^{CreER};EFNA5^{fl/fl}$ progeny. P2 neonates were treated with tamoxifen to cause deletion of *EFNA5* from $NG2^{+}$ cells (Figure S4D) and hindlimb muscles were subsequently examined histologically at P30. Similar to the muscle phenotypes of $NG2^{CreER};p65^{fl/fl}$, loss of *EFNA5* had no effect on myofiber number or the position of $NG2^{+}$ cells along the myofiber (Figure S4E, S4G), but did lead to a reduction in myonuclei number per fiber from multiple muscles, which was inversely correlated with an increase in interstitial nuclei (Figure 4C, 4D). To examine the ability of *EFNA5* to aid in myoblast migration, we simultaneously pulsed hindlimb muscles from $NG2^{CreER};EFNA5^{fl/fl}$ mice with BrdU and tamoxifen. EDL sections were prepared and the position of $BrdU^{+}$ myonuclei was then scored along the length of the muscle. The number of $BrdU^{+}$ myonuclei localized at the midline of EDL muscles was significantly reduced by 88% ($p = 0.07 \times 10^{-4}$) in $NG2^{CreER};EFNA5^{fl/fl}$ compared to $NG2^{CreER};EFNA5^{+/+}$ mice (Figure 4E and 4F). These findings phenocopy results obtained in $p65^{-/-}$ $NG2^{+}$ cells and suggest that *EFNA5* plays an important role in guiding the migration of myoblasts to the ends of growing myofibers. However, unlike $NG2^{CreER};p65^{fl/fl}$ mice, loss of *EFNA5* only trended to showing differences in the distribution of fiber diameter size (Figure S4F). Together, these results suggest that *EFNA5* is involved in regulating myoblast migration during neonatal muscle growth.

DISCUSSION

In our current study, we explored the underlying mechanism by which myoblasts migrate to their targeted myofibers. Our results revealed the involvement of an NF-κB signaling pathway functioning in an $NG2^{+}$ interstitial cell population. NF-κB is activated in these cells early in neonatal muscle development. Through its regulation of the ligand ephrinA5, $NG2^{+}$ cells contact and stimulate myoblasts to migrate towards the end of growing myofibers, where they subsequently fuse, thus providing an increased pool of myonuclei. In support of this notion, both deletion of *p65* and *EFNA5* from $NG2^{+}$ cells led to an increase in the

number of interstitial cells and a reduction in myonuclei compared to wild type mice. However, we noted that this phenotype did not occur to the same degree in all hindlimb muscles that we examined. This might be due to differences in when migration and accretion of myoblasts are at their maximum, or the ability of specific muscles to compensate for growth defects during neonatal development. It is also possible that failing to migrate to their proper location due to impaired signaling from $NG2^+$ cells, myoblasts may undergo a default pathway such as apoptosis leading to their turn over, which would affect their total numbers in the interstitium. We also observed that loss of *EFNA5* in $NG2^+$ cells did not affect the distribution of fiber size to the same extent as when *p65* was deleted from these same cells. Although it is possible that a difference in recombination efficiency of flox sites between *p65* and *EFNA5* alleles accounted for this variance, it is equally probable that, in addition to *EFNA5*, other NF-κB gene targets in $NG2^+$ cells are utilized to communicate with myoblasts and contribute in muscle growth.

Relatively little is known still how myoblast migrate. Global deletion of scatter factor/hepatocyte growth factor (SC/HGF) had originally been shown to cause a defect in the growth of developing limbs due to a failure in the migration of progenitor myoblasts (Bladt et al., 1995). A further role for the HGF/c-MET axis has been studied in adult muscles undergoing regeneration (Webster and Fan, 2013), but whether this ligand-receptor signaling pathway functions in newborn muscles to stimulate myoblast proliferation or migration is not known. Additional factors, CXCL12 and odorant receptor, MOR23, have also been shown to contribute to myoblast migration during *in vitro* myogenesis and adult muscle regeneration (Griffin et al., 2010; Griffin et al., 2009), but whether their activities are relevant in promoting myoblasts to the ends of growing fibers in newborn muscles will require additional investigation.

Ephrins/Eph signaling has previously been described in the regulation of axonal guidance, blood vessel formation, and neuromuscular junction maturation (Klein, 2012; Yumoto et al., 2008). Their expression has also been detected in normal and regenerating muscles, and selective ephrins have been shown to stimulate myoblast migration *in vitro* (Stark et al., 2011). However, in all of these instances, the upstream factors regulating Ephrin/Eph production have not been identified, nor has the *in vivo* context by which Ephrin/Eph signals regulate myoblasts or other cell types in skeletal muscle been resolved. Our findings demonstrate that one such upstream regulator is NF-κB, which functions as a direct transcriptional activator of *EFNA5*. Using a series of cell based and genetic approaches in mice, we further revealed that ephrinA5 expression in $NG2^+$ interstitial cells is necessary to promote cell-cell contact with myoblasts, which in turn stimulated myoblast migration. Because we found that $NG2^+$ cells are positioned along the length of a myofiber, whose locations were unaffected by the loss of p65 or ephrinA5, we envision that movement of myoblasts is likely to require multiple interactions with $NG2^+$ cells to reach the end of a developing fiber in newborn mice. The source of these myoblasts is currently unclear, but our results show that sub-laminar $Pax7^+$ cells stain positive for the proliferation marker Ki67 (Figure S4H), suggestive of activated satellite cells. Further immunohistochemical co-staining with dystrophin and laminin confirmed that such activation occurs within the niche where satellite cells reside (Figure S4I). These results indicate that during neonatal muscle

growth, satellite cells represent at least one cell type that contribute to the myoblast pool involved in migration and fusion to growing myofibers.

As opposed to adult muscle injury where macrophages and resident mesenchymal progenitor cells have been shown to contribute to a pro-regenerative response (Deng et al., 2012; Joe et al., 2010), the role that stromal cells play in regulating the growth of newborn muscles has been much less appreciated. Only recently has a population of connective tissue fibroblasts expressing the transcription factor, Tcf4, been linked to the maturation of neonatal muscle by regulating the specification of fiber type, potentially through a secreted factor whose cell of origin remains to be elucidated (Mathew et al., 2011). Here, our current work adds to the unique role of a muscle interstitial cell population whose communication with myoblasts plays a key role in neonatal muscle growth.

EXPERIMENTAL PROCEDURES

Mice

All animals were housed, maintained, and used according to protocols approved by the Institutional Animal Care and Use committees (IACUC) at the Ohio State University. *NF-κB*$^{EGFP/+}$, *Rosa26-Tomato*, *iNOS*$^{-/-}$, *NG2*^{CreER}, and *p50*$^{-/-}$ mice were purchased from Jackson Laboratories. *p65*$^{-/-}$*;TNFRα*$^{-/-}$ and *p65*$^{fl/fl}$ *mice* were generated as previously described (Doi et al., 1999; Steinbrecher et al., 2008). The EFNA5 cKO (*Efna5*$^{fl/fl}$) mouse was generated using standard Embryonic Stem Cell technology (Tessarollo et al., 2009). The targeting vector was obtained from the International Mouse Knockout Consortium (IKMC). Correctly recombined ES cells were identified by Southern analysis. Germline transmission of the targeted allele (IKMC tm1a allele) was assessed by PCR according to IKMC guidelines. Before use for indicated experiments, *Efna5*$^{tm1a/+}$ mice were bred to a ubiquitous *Flpe* strain (Jackson Laboratories). In the *Efna5*$^{tm1c/+}$ (*Efna5*$^{fl/+}$) mice, excision of the IRES-LacZ-neo cassette was verified by PCR using the suggested IKMC primers. *NG2*^{CreER} mice (Jackson Laboratories) were crossed with *p65*$^{fl/fl}$ *or EFNA*$^{fl/fl}$ to delete *p65 or EFNA5* in NG2^{+} cells. To induce recombination in early neonatal development, tamoxifen (0.2 mg/pup) dissolved in corn oil was injected subcutaneously to postnatal day 2 (P2) mice.

Immunofluorescence Staining

Muscle tissues were snap frozen with O.C.T. in methyl-butane solutions chilled in liquid nitrogen. To freeze muscle containing EGFP or Tomato reporter, muscle tissues were prefixed with 4% paraformaldehyde, overnight at 4°C followed by a 48h incubation with 30% sucrose at 4°C. For EGFP^{+} ISC analysis, whole hindlimbs were used from P7 mice, otherwise Quad and Gas muscles were used from mice at P14 or older. 10μm sections were obtained for all staining experiment except for myonuclei number/fiber counting using 30μm-thick sections. Sections were air-dried and incubated with 4% paraformaldehyde for fixation at room temperature, followed by incubation with blocking buffer containing 5% goat serum and 0.2% triton X-100 for 30min at room temperature. Primary antibodies: anti-NG2 (Millipore), anti-CD31 (BD Pharmingen), anti-α laminin (Sigma), anti-MyoD (Dako) were diluted in blocking buffer and incubated for 1h at room temperature. For MyoD, the

primary antibody was incubated for overnight at 4°C. After washing three times with PBS, fluorescent-conjugated secondary antibodies (Invitrogen) were incubated for 1h at room temperature. The slides were rinsed with PBS and stained with DAPI solutions. For adherent cell staining, culture plates were washed with PBS and directly fixed with 4% paraformaldehyde. Anti-ki67 (Dako) and anti-troponin T (Sigma) were used as primary antibodies following the same procedure as described for tissue sections. The images were obtained with either an Olympus FV 1000 Spectral or filter confocal laser microscope and analyzed by Image J and FV10-ASW 4.0 viewer. At least three mice were analyzed for each staining.

Statistical Analysis

All quantitative data was shown as mean ± s.e.m. All statistical analysis were performed by using 2-tailed unpaired Student's *t* test. (*) $p < 0.05$, (**) $p < 0.01$, (***) $p< 0.001$.

Supplementary Material

Refer to Web version on PubMed Central for supplementary material.

ACKNOWLEDGMENTS

We thank A. Baldwin and A. Beg for generously providing mice, A. Selen Yilmaz for assistance with additional Bioinformatics, the Pollock lab and S. Cole for technical assistance for live cell imaging, and M. Viapiano for assistance with the two-chamber migration system. We also thank G. Leone, M. Ostrowski, the S. Amacher laboratory, and F. Montanaro for their interactions, and M. Campion in the Guttridge laboratory for assistance with whole-mount staining, as well as other members of Guttridge laboratory for engaging discussions throughout the course of this study. This project was supported by an NIH grant, 2R01 AR052787 to D.C.G.

REFERENCES

Bladt F, Riethmacher D, Isenmann S, Aguzzi A, Birchmeier C. Essential role for the c-met receptor in the migration of myogenic precursor cells into the limb bud. Nature. 1995; 376:768–771. [PubMed: 7651534]

Braun T, Gautel M. Transcriptional mechanisms regulating skeletal muscle differentiation, growth and homeostasis. Nat Rev Mol Cell Biol. 2011; 12:349–361. [PubMed: 21602905]

Britto PR, Perez-Escamilla R. No second chances? Early critical periods in human development. Introduction. Social science & medicine. 2013; 97:238–240. [PubMed: 24084209]

Cappellari O, Cossu G. Pericytes in development and pathology of skeletal muscle. Circ Res. 2013; 113:341–347. [PubMed: 23868830]

Dahlman JM, Bakkar N, He W, Guttridge DC. NF-kappaB functions in stromal fibroblasts to regulate early postnatal muscle development. J Biol Chem. 2010; 285:5479–5487. [PubMed: 20018862]

Davis TA, Fiorotto ML. Regulation of muscle growth in neonates. Curr Opin Clin Nutr Metab Care. 2009; 12:78–85. [PubMed: 19057192]

Dellavalle A, Maroli G, Covarello D, Azzoni E, Innocenzi A, Perani L, Antonini S, Sambasivan R, Brunelli S, Tajbakhsh S, et al. Pericytes resident in postnatal skeletal muscle differentiate into muscle fibres and generate satellite cells. Nature communications. 2011; 2:499.

Deng B, Wehling-Henricks M, Villalta SA, Wang Y, Tidball JG. IL-10 triggers changes in macrophage phenotype that promote muscle growth and regeneration. J Immunol. 2012; 189:3669–3680. [PubMed: 22933625]

Doi TS, Marino MW, Takahashi T, Yoshida T, Sakakura T, Old LJ, Obata Y. Absence of tumor necrosis factor rescues RelA-deficient mice from embryonic lethality. Proc Natl Acad Sci. 1999; 96:2994–2999. [PubMed: 10077625]

Ehler E, Gautel M. The sarcomere and sarcomerogenesis. Adv Exp Med Biol. 2008; 642:1–14. [PubMed: 19181089]

Griffin CA, Apponi LH, Long KK, Pavlath GK. Chemokine expression and control of muscle cell migration during myogenesis. Journal of cell science. 2010; 123:3052–3060. [PubMed: 20736301]

Griffin CA, Kafadar KA, Pavlath GK. MOR23 promotes muscle regeneration and regulates cell adhesion and migration. Dev Cell. 2009; 17:649–661. [PubMed: 19922870]

Hayden MS, Ghosh S. Signaling to NF-kappaB. Genes Dev. 2004; 18:2195–2224. [PubMed: 15371334]

Hayden MS, Ghosh S. NF-kappaB, the first quarter-century: remarkable progress and outstanding questions. Genes Dev. 2012; 26:203–234. [PubMed: 22302935]

Joe AW, Yi L, Natarajan A, Le Grand F, So L, Wang J, Rudnicki MA, Rossi FM. Muscle injury activates resident fibro/adipogenic progenitors that facilitate myogenesis. Nat Cell Biol. 2010; 12:153–163. [PubMed: 20081841]

Kitiyakara A, Angevine DM. A Study of the Pattern of Postembryonic Growth of M. Gracilis in Mice. Dev Biol. 1963; 8:322–340. [PubMed: 14084729]

Klein R. Eph/ephrin signalling during development. Development. 2012; 139:4105–4109. [PubMed: 23093422]

Li J, Johnson SE. Ephrin-A5 promotes bovine muscle progenitor cell migration before mitotic activation. J Anim Sci. 2013; 91:1086–1093. [PubMed: 23296833]

Magness ST, Jijon H, Van Houten Fisher N, Sharpless NE, Brenner DA, Jobin C. In vivo pattern of lipopolysaccharide and anti-CD3-induced NF-kappa B activation using a novel gene-targeted enhanced GFP reporter gene mouse. Journal of immunology. 2004; 173:1561–1570.

Mathew SJ, Hansen JM, Merrell AJ, Murphy MM, Lawson JA, Hutcheson DA, Hansen MS, Angus-Hill M, Kardon G. Connective tissue fibroblasts and Tcf4 regulate myogenesis. Development. 2011; 138:371–384. [PubMed: 21177349]

Petrie RJ, Doyle AD, Yamada KM. Random versus directionally persistent cell migration. Nature reviews Molecular cell biology. 2009; 10:538–549. [PubMed: 19603038]

Poliakov A, Cotrina M, Wilkinson DG. Diverse roles of eph receptors and ephrins in the regulation of cell migration and tissue assembly. Dev Cell. 2004; 7:465–480. [PubMed: 15469835]

Siegel AL, Atchison K, Fisher KE, Davis GE, Cornelison DD. 3D timelapse analysis of muscle satellite cell motility. Stem cells. 2009; 27:2527–2538. [PubMed: 19609936]

Stark DA, Karvas RM, Siegel AL, Cornelison DD. Eph/ephrin interactions modulate muscle satellite cell motility and patterning. Development. 2011; 138:5279–5289. [PubMed: 22071104]

Steinbrecher KA, Harmel-Laws E, Sitcheran R, Baldwin AS. Loss of epithelial RelA results in deregulated intestinal proliferative/apoptotic homeostasis and susceptibility to inflammation. J Immunol. 2008; 180:2588–2599. [PubMed: 18250470]

Swartz ME, Eberhart J, Pasquale EB, Krull CE. EphA4/ephrin-A5 interactions in muscle precursor cell migration in the avian forelimb. Development. 2001; 128:4669–4680. [PubMed: 11731448]

Tessarollo L, Palko ME, Akagi K, Coppola V. Gene targeting in mouse embryonic stem cells. Methods Mol Biol. 2009; 530:141–164. [PubMed: 19266325]

Webster MT, Fan CM. c-MET regulates myoblast motility and myocyte fusion during adult skeletal muscle regeneration. PloS one. 2013; 8:e81757. [PubMed: 24260586]

White RB, Bierinx AS, Gnocchi VF, Zammit PS. Dynamics of muscle fibre growth during postnatal mouse development. BMC Dev Biol. 2010; 10:21. [PubMed: 20175910]

Williams PE, Goldspink G. Longitudinal growth of striated muscle fibres. J Cell Sci. 1971; 9:751–767. [PubMed: 5148015]

Yumoto N, Wakatsuki S, Kurisaki T, Hara Y, Osumi N, Frisen J, Sehara-Fujisawa A. Meltrin beta/ADAM19 interacting with EphA4 in developing neural cells participates in formation of the neuromuscular junction. PloS one. 2008; 3:e3322. [PubMed: 18830404]

Highlights

- NF-κB is activated in $NG2^+$ interstitial cells in neonatal skeletal muscle.
- NF-κB functions in $NG2^+$ interstitial cells to promote myoblast migration.
  - The gene encoding EphrinA5 is a direct target of NF-kB.
    - EphrinA5 from $NG2^+$ interstitial cells promotes myoblast migration.

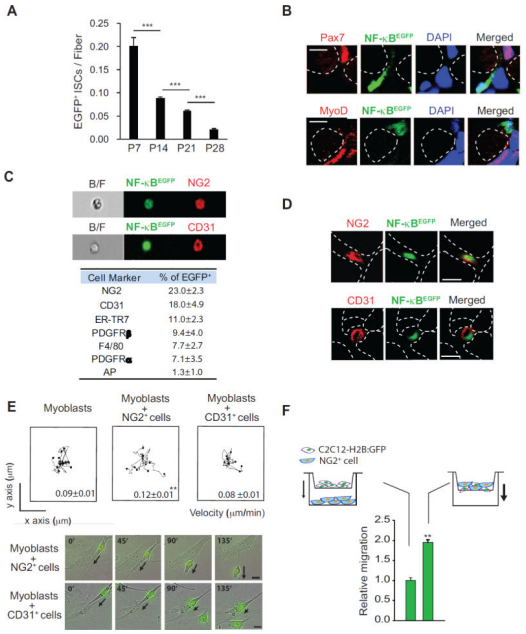

Figure 1. NF-κB Localizes to NG2$^+$ Cells during Neonatal Skeletal Muscle Development

(**A**) Muscle sections were prepared from *NFκB-EGFP* mice at P7, P14, P21, and P28 for laminin staining. EGFP$^+$ interstitial cells (ISCs) located outside of laminin were counted per cross sectional area and normalized to fiber numbers. Error bars indicate SEM. ***p < 0.001. (**B**) Muscle sections from P7 *NFκB-EGFP* mice were analyzed for Pax7 (top, red) or MyoD (bottom, red) and NFκB (green) positive cells. Dotted white cells represent myofiber boundaries. DAPI was used for nuclear staining. (**C**) Representative images of NG2$^+$ EGFP$^+$ (top) and CD31$^+$ EGFP$^+$ cells (bottom) from the FACS analysis. Table generated from FACS analysis summarizing the percentage of mononuclear cells from P7 *NFκB-EGFP* mice expressing EGFP and indicated cell surface markers used to identify cell types. (**D**) Muscle sections from P7 *NFκB-EGFP* mice were analyzed for cell expressing both EGFP and NG2 (top) or CD31 (bottom). Dotted white cells represent myofiber boundaries. **(E)** C2C12-H2B:GFP myoblasts were co-cultured with NG2 or CD31 positive cells isolated from P2 – P5 wild type mice, and then recorded for 10h using time lapse fluorescence microscopy (top). The migration of C2C12-H2B:GFP myoblasts was measured after contacting with CD31$^+$ or NG2$^+$ cells and the data are presented as mean ± s.e.m. Representative still shots from the time-lapse fluorescence microscopy are shown (bottom). Arrows indicate the movements of C2C12-H2B:GFP myoblasts. (**F**) Migration of C2C12-H2B:GFP myoblasts was monitored using a Boyden chamber system where NG2$^+$ cells were plated either in the lower chamber alone (left) or added to the upper chamber (right) at a 1:1 ratio with C2C12-H2B:GFP myoblasts. Relative migration was normalized to C2C12-H2B:GFP myoblasts migration by themselves. B/F: bright field image. Scale bars = 5 μm (**B**) and 10 μm (**D**) and (**E**). ***p < 0.01* by the student's *t*-test. See accompanying Figure S1 and Movie S1. Error bars, SEM

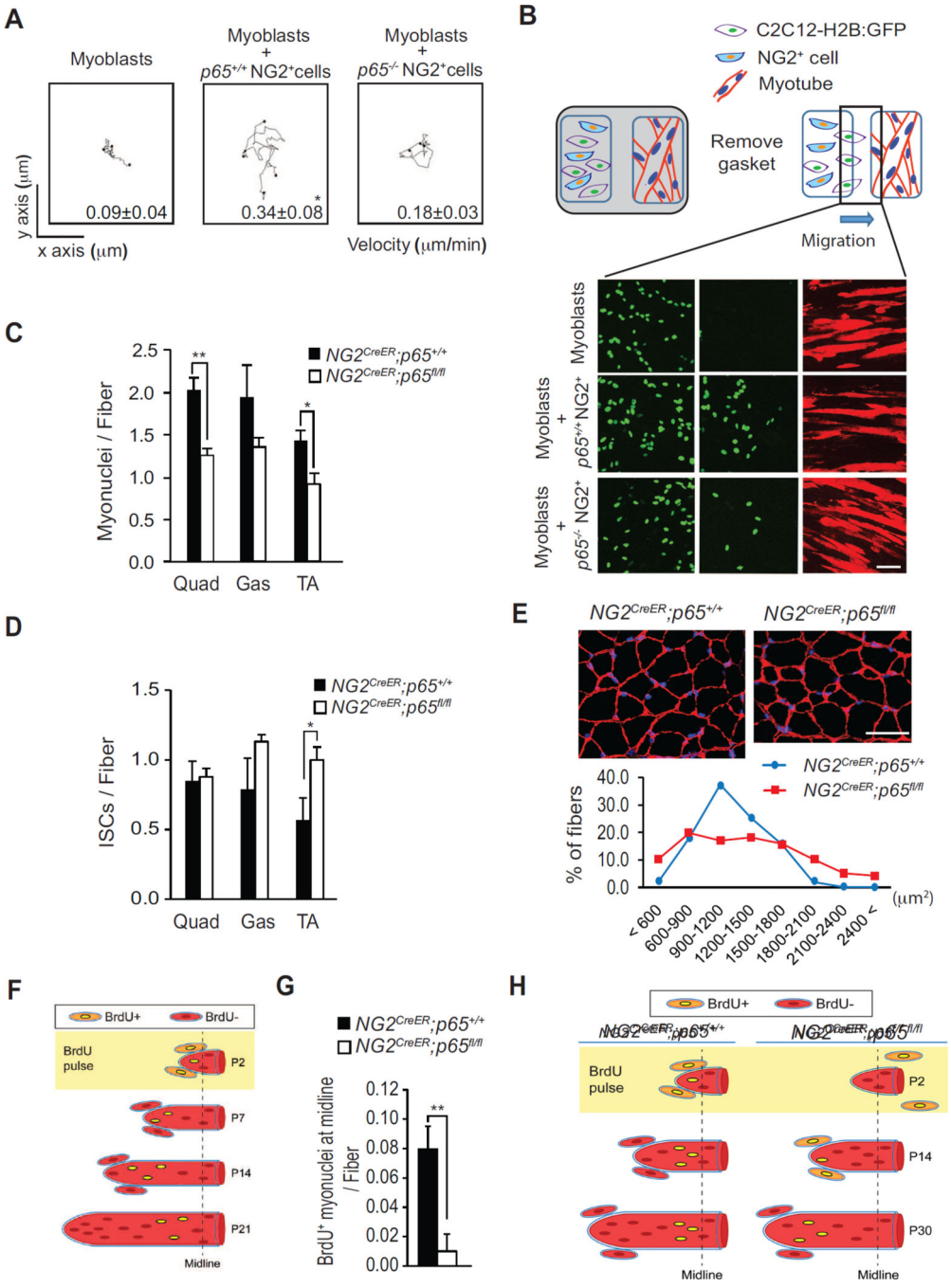

Figure 2. The p65 Activity of NF-κB Functions in NG2 Cells to Promote Myoblast Migration *in vitro* and *in vivo*

(**A**) Plots of time-lapse microscopy, recording the migration of C2C12-H2B:GFP myoblasts cultured alone, or with either $p65^{+/+}$ $NG2^{+}$, or with $p65^{-/-}$ $NG2^{+}$ cells. The migration of C2C12-H2B:GFP myoblasts was measured following there contact with $p65^{+/+}$ or $p65^{-/-}$ $NG2^{+}$ cells. Values are presented as mean ± s.e.m. (**B**) Two-chamber migration system showing differentiated C2C12 myotubes (red) on the right side of the chamber and C2C12-H2B:GFP myoblasts (green) on the left side cultured either alone, with $p65^{+/+}$ $NG2^{+}$ cells,

or with $p65^{-/-}$ $NG2^{+}$ cells. Upon removal of the gasket, C2C12-H2B:GFP myoblasts migrate towards myotubes and cell number was scored across the gap at 24h. Relative migration was expressed as mean ± s.e.m. Myotubes were visualized by immunostaining for Troponin T. (**C**) Myonuclei number per fiber was measured from quadriceps (Quad), gastrocnemius muscles (Gas) and tibialis anterior (TA) muscles from $NG2^{CreER};p65^{+/+}$ and $NG2^{CreER};p65^{fl/fl}$ mice. Approximately, 800 myonuclei for each genotypes were analyzed. (**D**) $DAPI^{+}$ interstitial cells (ISCs) were measured from Quad, Gas, and TA muscles from P30 $NG2^{CreER};p65^{+/+}$ and $NG2^{CreER};p65^{fl/fl}$ mice. (**E**) (top) Representative cross sections of Gas from P30 $NG2^{CreER};p65^{+/+}$ and $NG2^{CreER};p65^{fl/fl}$ mice immunostained for laminin and counterstained with DAPI. (bottom) Quantitative distribution of fiber size from $NG2^{CreER};p65^{+/+}$ and $NG2^{CreER};p65^{fl/fl}$ mice recorded from a minimum of 1000 fibers. (**F**) Schematic of BrdU injection experiment where $BrdU^{+}$ cells are depicted with yellow nuclei. (**G**) BrdU was injected in P2 $NG2^{CreER};p65^{+/+}$ and $NG2^{CreER};p65^{fl/fl}$ mice, and at P30 EDL muscle sections were analyzed for the sublaminar localization of $BrdU^{+}$ cells per myofiber, measured at the midline of the muscle. (**H**) A model for $BrdU^{+}$ cell accretion in EDL muscles from $NG2^{CreER};p65^{+/+}$ and $NG2^{CreER};p65^{fl/fl}$ mice. Scale bars = 100 μm for (**B**) and (**C**). $*p < 0.05$, $**p < 0.01$ by the student's *t*-test. See accompanying Figure S2; Movie S2, and Movie S3. Error bars, SEM

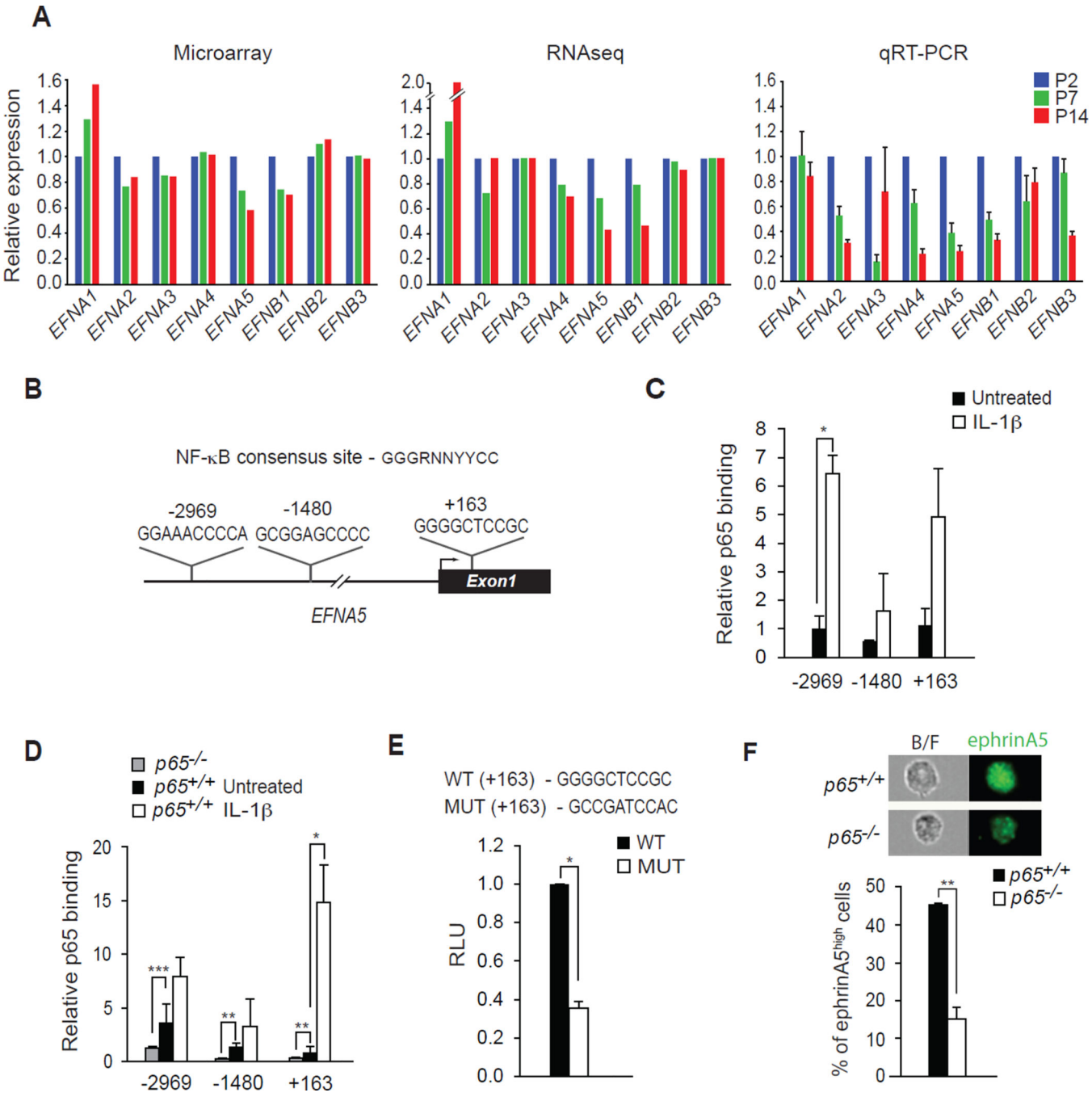

Figure 3. *EFNA5* is Transcriptionally Regulated by NF-κB

(**A**) Microarray, RNAseq, and quantitative RT-PCR were performed probing for the expression of ephrin genes from skeletal muscles at P2, P7, and P14. (**B**) A schematic map of the 5' region of the *EFNA5* gene and locations of conserved NF-κB DNA binding sites at −2969, −1480, and +163 relative to the transcriptional start site. (**C**) ChIP assays for p65 binding to the *EFNA5* promoter in $NG2^{+}$ cells untreated and treated with 10 ng/ml of IL-1β. (**D**) ChIP assays for p65 binding to the *EFNA5* promoter in $p65^{+/+}$ MEFs untreated and treated with 10 ng/ml of IL-1β, compared with untreated $p65^{-/-}$ MEFs *** $p < 0.001$. (**E**) A

portion of *EFNA5* gene containing the +163 binding site of NF-κB was cloned into a luciferase reporter construct. Luciferase activity was measured following the transfection of an *EFNA5* promoter reporter construct in MEFs, and compared to activity generated from an *EFNA5* promoter reporter construct containing a mutation in the +163 NF-κB binding site. (**F**) Representative flow images of ephrinA5 from $p65^{+/+}$ and $p65^{-/-}$ NG2 cells (top). Percentage of ephrinA5^{high} NG2 cells isolated from $p65^{+/+}$ and $p65^{-/-}$ cells (bottom). RLU: Relative Luciferase Units. B/F: bright field image. *$p < 0.05$, **$p < 0.01$ by the student's *t*-test. See accompanying Figure S3. Error bars, SEM

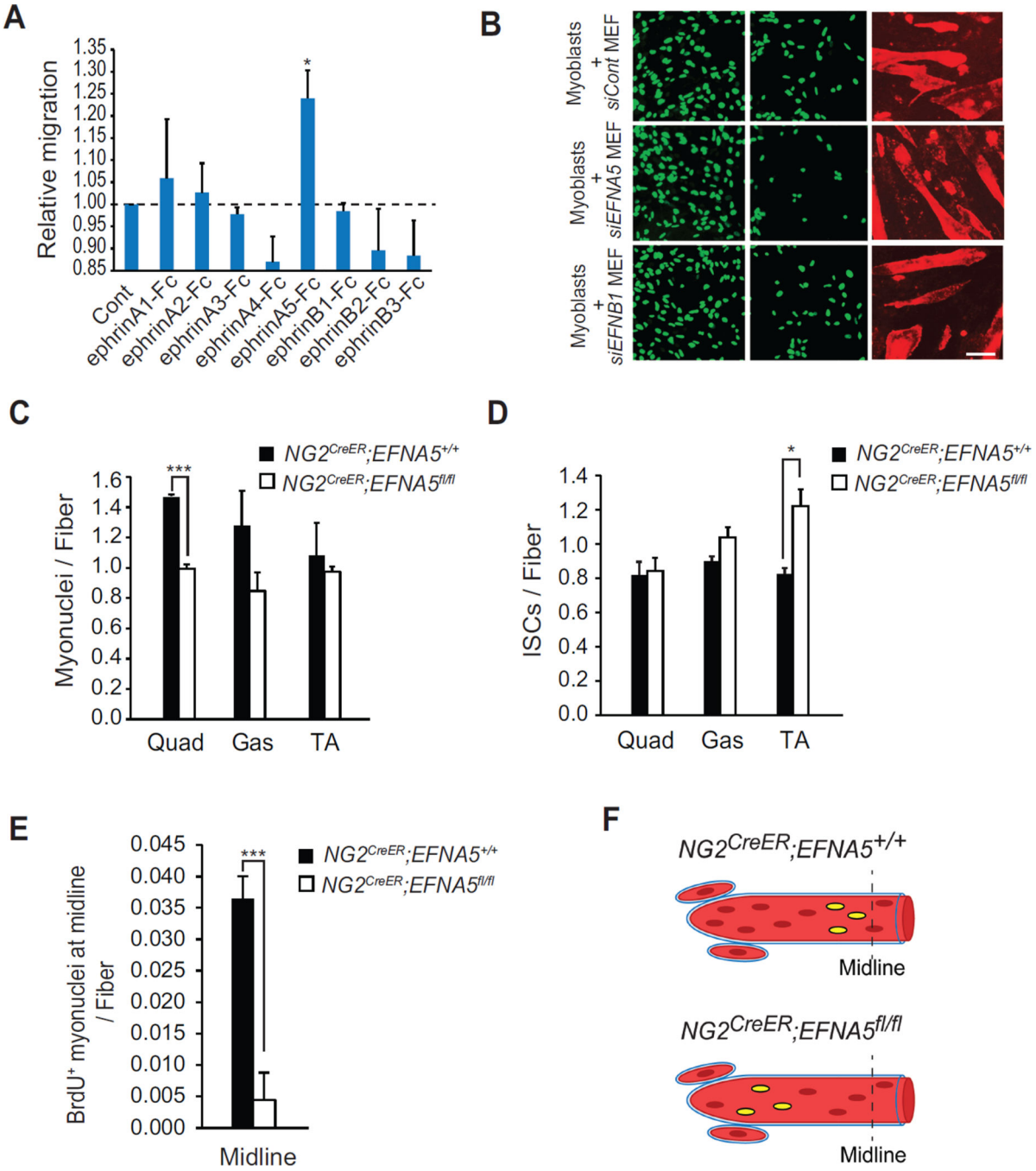

Figure 4. *EFNA5* from NG2^{+} Cells Mediates Myoblast Migration *in vitro* and *in vivo*

(**A**) A Boyden chamber was used to measure migration of myoblasts when exposed for 24h to different recombinant Fc-clustered ephrins. (**B**) A two-chamber assay system was used to measure migration of C2C12-H2B:GFP myoblasts toward myotubes when co-cultured with MEFs transfected with siRNAs against *EFNA5* or *EFNB1*. Relative migration is shown as mean ± s.e.m. Myonuclei number per fiber (**C**) and DAPI^{+} ISCs (**D**) was measured from Quad, Gas and TA muscles from P30 *NG2^{CreER};EFNA5$^{+/+}$* and *NG2^{CreER};EFNA5$^{fl/fl}$* mice. (**E**) BrdU was injected in *NG2^{CreER};EFNA5$^{+/+}$* and *NG2^{CreER};EFNA5$^{fl/fl}$* mice and at P30

muscle sections were analyzed for the sublaminar localization of $BrdU^+$ cells at the midline of EDL muscles. (**F**) A model for $BrdU^+$ cell accretion in muscles from $NG2^{CreER};EFNA5^{+/+}$ and $NG2^{CreER};EFNA5^{fl/fl}$ mice. Scale bars = 100 μm for (**B**) $*p < 0.05$, $***p < 0.001$ by the student's *t*-test. See accompanying Figure S4. Error bars, SEM